The International Conference of Computational Methods
April 4–6, 2007, Hiroshima

A C^0 DISCONTINUOUS GALERKIN FORMULATION FOR THIN SHELLS

N. T. Dung, G. N. Wells

Faculty of Civil Engineering and Geosciences
Delft University of Technology, Stevinweg 1, 2628 CN Delft, Netherlands
d.nguyentien@tudelft.nl, g.n.wells@tudelft.nl

Abstract

This paper presents a C^0 discontinuous Galerkin formulation for the simulation of thin shells. The method is based on Koiter's shell model and allows finite element solutions to be obtained by using standard C^0 Lagrange basis functions in terms of the displacement only. It invokes a curvature-like term by applying a lifting operation which transforms jumps in the normal rotation across element boundaries into a field defined on element interiors. This procedure enforces weak continuity of normal derivative across element boundaries and a special term is added to enhance stability of the formulation. Benchmark tests using various-order elements are presented and conclusions are drawn as to the computational efficiency of the method.

Keywords: Shells, discontinuous Galerkin methods, Koiter's shell model, rotation-free.

1 Introduction

For the numerical simulation of thin shells, many shell elements have been proposed and developed over the years. These are copious in quantity, but are in general all built upon one of two shell theory families, namely the Koiter and Naghdi families. While the former ignores transverse shear effects by applying the Kirchhoff-Love kinematic assumptions, the latter is based on the Reissner-Mindlin kinematic assumptions and takes transverse shear effects into account [1, 2]. Conventionally, the Koiter type model requires the use of C^1 basis functions, which are difficult to construct, while the Naghdi-type model demands the use of C^0 functions. Because of its simple implementation, the Naghdi-type model is attractive, although it poses some other difficulties, particularly shear locking when shell thickness becomes small.

Recently, some discontinuous Galerkin formulations have been presented for the simulating of thin bending problems. In the works of Engel et al. [3] and Hughes and Garikipati [4], a C^0 interior-penalty formulation for Kirchhoff plates that permits the use standard C^0 Lagrange finite element basis functions has been proposed. With this formulation, rotation degrees of freedom are not required and continuity of normal slope across element boundaries is enforced weakly. Althought the approach is relatively simple, it has drawbacks, such as conditional stability and ambiguities for nonlinear implementations. To address these issues, Wells and Dung [5] recently developed a C^0 discontinuous Galerkin formulation for Kirchhoff plates which are inspired by the works of Bassi and Rebay [6] and Brezzi et al. [7] for second-order problems. The approach relies on a lifting operation that transforms jumps in the normal rotation across element boundaries into a field defined on element interiors. The stability of the approach can be precisely quantified and the extention to nonlinear problems is straight-forward. In this paper, we develop a C^0 discontinuous Galerkin formulation from the Koiter shell model based upon this approach.

We organize the remainder of this work as follows: firstly, equations for the Koiter shell model are summarized in Section 2. Then, in Section 3, the considered formulation for thin shells is presented, after which numerical examples are presented in Section 4. Finally, conclusions are drawn in Section 5.

2 Thin shell formulation

Formulations for thin shell finite-element analysis have been presented and developed by numerous authors, including Koiter and Simmonds [8], Bernadou [1] and Chapelle and Bathe [2]. In this section, equations for Koiter's shell model are summarized. We shall restrict our attention on linear problems, and adopt largely the notation of Bernadou [1] and Chapelle and Bathe [2].

2.1 Kinematic equations

Consider a shell with a mid-surface denoted by S and with thickness t. The boundary is denoted ∂S, and the shell lies in an orthonormal coordinate system $(\boldsymbol{e}^1, \boldsymbol{e}^2, \boldsymbol{e}^3)$. The mid-surface of the given shell is defined by an injectively geometric mapping from a parametric space R^2 into the Euclidean space E^3 (see Figure 1). Denote the reference domain in the space R^2 by Ω and its boundary by $\partial\Omega$ that their images in the space E^3 are S and ∂S, respectively. Consider a coordinate system (ξ^1, ξ^2, ξ^3) that (ξ^1, ξ^2) is a

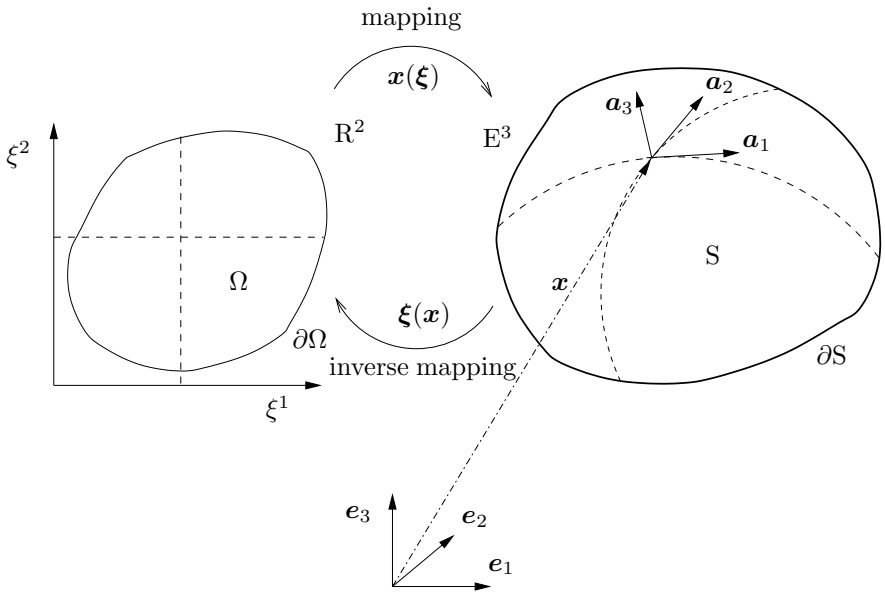

Figure 1: Definition of shell geometry.

point on Ω and $\boldsymbol{x}\left(\xi^1,\xi^2\right)$ is the position vector of its image on the mid-surface. The surface covariant basis vectors are now defined as:

$$\boldsymbol{a}_\alpha = \frac{\partial \boldsymbol{x}}{\partial \xi^\alpha}, \qquad\qquad \boldsymbol{a}_3 = \frac{\boldsymbol{a}_1 \times \boldsymbol{a}_2}{\|\boldsymbol{a}_1 \times \boldsymbol{a}_2\|}, \tag{1}$$

where $\alpha = 1,2$ are indices denotting two directions of the surface tangent plane at the point. The surface contravariant basis vectors $\boldsymbol{a}^\alpha$ are defined by the relation $\boldsymbol{a}_\beta \cdot \boldsymbol{a}^\alpha = \delta^\alpha_\beta$, where δ^α_β is the Kronecker delta tensor. Now, covariant components $a_{\alpha\beta}$ and contravariant-covariant components a^α_β of the metric tensor are defined as

$$a_{\alpha\beta} = \boldsymbol{a}_\alpha \cdot \boldsymbol{a}_\beta, \qquad\qquad a^\alpha_\beta = \boldsymbol{a}^\alpha \cdot \boldsymbol{a}_\beta. \tag{2}$$

They are also called the first fundamental form of the mid-surface. Components of the second fundamental form containing the curvature information of the mid-surface are defined as

$$b_{\gamma\alpha} = -\mathrm{a}_{3,\alpha} \cdot \mathrm{a}_\gamma, \qquad\qquad b^\gamma_\alpha = -\mathrm{a}_{3,\alpha} \cdot \mathrm{a}^\gamma. \tag{3}$$

Herein, some other geometric definitions of the mid-surface are used, that include

$$\Gamma^\delta_{\gamma\alpha} = -\mathrm{a}^\delta_{,\alpha} \cdot \mathrm{a}_\gamma, \tag{4}$$

namely the surface Christoffel symbols, and

$$a = \det\left(a_{\alpha\beta}\right) \tag{5}$$

appearing in the relation $dS = \sqrt{a}\; d\Omega$. The position vector $\boldsymbol{x}^p$ of a material point in the shell media relates to the position vector $\boldsymbol{x}$ on the mid-surface as the following:

$$\boldsymbol{x}^p\left(\xi^1,\xi^2,\xi^3\right) = \boldsymbol{x}\left(\xi^1,\xi^2\right) + \xi^3 \boldsymbol{a}_3\left(\xi^1,\xi^2\right). \tag{6}$$

Under the external loads, the structure deforms. Denote the displacement vectors at a material point and at a mid-surface point by $\boldsymbol{u}$ and $\boldsymbol{u}^p$, respectively. The relation between them reads:

$$\boldsymbol{u}^p\left(\xi^1,\xi^2,\xi^3\right) = \boldsymbol{u}\left(\xi^1,\xi^2\right) + \xi^3 \theta_\alpha\left(\xi^1,\xi^2\right) \boldsymbol{a}^\alpha\left(\xi^1,\xi^2\right), \tag{7}$$

where θ_α are rotations around the two directions on the tangent plane of a material line which is normal to the mid-surface in the undeformed state. In the equation (7), the Kirchhoff-Love kinematic assumptions mentioning about straight and un-stretched material lines have been adopted. Furthermore, the assumptions also state that material lines are always orthogonal to the mid-surface, that results in:

$$\theta_\alpha = -u_{3,\alpha} - b_\alpha^\delta u_\delta. \tag{8}$$

Applying the above relations, the strain tensor at a material point is expressed as

$$\epsilon_{\alpha\beta} = \gamma_{\alpha\beta} - \xi^3 \kappa_{\alpha\beta}. \tag{9}$$

The membrane part $\gamma_{\alpha\beta}$ in the above equation reads

$$\gamma_{\alpha\beta} = \frac{1}{2}\left(u_{\alpha|\beta} + u_{\beta|\alpha}\right) - b_{\alpha\beta}\, u_3, \tag{10}$$

where $u_{\alpha|\beta}$ is called the covariant derivative of the displacement component u_α, which is expressed as

$$u_{\alpha|\beta} = u_{\alpha,\beta} - \Gamma_{\alpha\beta}^\gamma\, u_\gamma. \tag{11}$$

The curvature $\kappa_{\alpha\beta}$ in the equation (9) is given by

$$\kappa_{\alpha\beta} = u_{3|\alpha\beta} + b_{\alpha|\beta}^\gamma\, u_\gamma + b_\alpha^\gamma u_{\gamma|\beta} + b_\beta^\gamma u_{\gamma|\alpha} - b_\alpha^\gamma b_{\gamma\beta}, \tag{12}$$

where the covariant derivatives $u_{3|\alpha\beta}$ and $b_{\alpha|\beta}^\gamma$ are defined as

$$u_{3|\alpha\beta} = u_{3,\alpha\beta} - \Gamma_{\alpha\beta}^\gamma\, u_{3,\gamma}, \tag{13}$$

$$b_{\alpha|\beta}^\gamma = b_{\alpha,\beta}^\gamma + \Gamma_{\beta\delta}^\gamma\, b_\alpha^\delta - \Gamma_{\alpha\beta}^\delta\, b_\delta^\gamma. \tag{14}$$

The above equations permit the strain tensors at a material point in the shell medium to be expressed in terms of the displacement field defined on the two-dimensional reference domain Ω.

2.2 Variational form

The boundary $\partial\Omega$ of the domain Ω is partitioned such that $\overline{\Gamma^u \cup \Gamma^H} = \overline{\Gamma^\theta \cup \Gamma^M} = \partial\Omega$ and $\Gamma^u \cap \Gamma^H = \Gamma^\theta \cap \Gamma^M = \emptyset$. The distributed force vector on Ω is denoted by $\boldsymbol{F}$, the displacement, rotation, force, and moment vectors on the boundaries are denoted by $\boldsymbol{g}^u$, $\boldsymbol{g}^\theta$, $\boldsymbol{H}$, and $\boldsymbol{M}$, respectively. Note that $\boldsymbol{F}$, $\boldsymbol{g}^u$, $\boldsymbol{g}^\theta$, $\boldsymbol{H}$, and $\boldsymbol{M}$ have been evaluated by an inverse map from the physical space into the reference space. The spaces of trial and test functions on the mid-surface are defined as follows:

$$U = \left\{\boldsymbol{u} = (u_\alpha, u_3) \in [H^1(\Omega)]^2 \times H^2(\Omega) : \boldsymbol{u}|_{\Gamma^u} = \boldsymbol{g}^u,\ \boldsymbol{\theta}\left(\boldsymbol{u}\right)|_{\Gamma^\theta} = \boldsymbol{g}^\theta\right\}, \tag{15}$$

$$W = \left\{\boldsymbol{w} = (w_\alpha, w_3) \in [H^1(\Omega)]^2 \times H^2(\Omega) : \boldsymbol{w}|_{\Gamma^u} = \boldsymbol{0},\ \boldsymbol{\theta}\left(\boldsymbol{w}\right)|_{\Gamma^\theta} = \boldsymbol{0}\right\}. \tag{16}$$

In order to provide a two-dimensional presentation of a three-dimensional shell medium, integrals with respect to the thickness direction in the variational form derived from the kinetic equation are evaluated in advance. This process results the following variational form: find $\boldsymbol{u} \in U$ such that

$$B\left(\boldsymbol{w}, \boldsymbol{u}\right) = L\left(\boldsymbol{w}\right) \quad \forall \boldsymbol{w} \in \mathcal{W}, \tag{17}$$

where

$$B\left(\boldsymbol{w},\boldsymbol{u}\right)=\int_{\Omega}\left\{t\gamma_{\alpha\beta}\left(\boldsymbol{w}\right)\mathcal{C}^{\alpha\beta\gamma\delta}\gamma_{\gamma\delta}\left(\boldsymbol{u}\right)+\frac{t^{3}}{12}\kappa_{\alpha\beta}\left(\boldsymbol{w}\right)\mathcal{C}^{\alpha\beta\gamma\delta}\kappa_{\gamma\delta}\left(\boldsymbol{u}\right)\right\}\sqrt{a}\;d\Omega, \quad (18)$$

$$L\left(\boldsymbol{w}\right)=\int_{\Omega}\boldsymbol{w}\cdot\boldsymbol{F}d\Omega+\int_{\Gamma^{H}}\boldsymbol{w}\cdot\boldsymbol{H}\;d\Gamma+\int_{\Gamma^{M}}\boldsymbol{\theta}\left(\boldsymbol{w}\right)\cdot\boldsymbol{M}\;d\Gamma, \quad (19)$$

and $C^{\alpha\beta\gamma\delta}$ is the fourth-order constitutive tensor on the shell mid-surface. In the isotropic case, it is defined as

$$\mathcal{C}^{\alpha\beta\gamma\delta}=\frac{E}{2\left(1+\nu\right)}\left(a^{\alpha\gamma}a^{\beta\delta}+a^{\alpha\delta}a^{\beta\gamma}+\frac{2\nu}{1-\nu}a^{\alpha\beta}a^{\gamma\delta}\right). \quad (20)$$

where E denotes Young's modulus and ν denotes Poisson's ratio. The variational form (17) is expressed in terms of the displacement field and its derivatives in the reference coordinat system (ξ^1,ξ^2). For a conventional finite element approach, the requirement of C^0 continuity for the membrane deformation is straightforward, but for bending part, a comforming C^1 continuity is difficult to construct. In the next section, a C^0 discontinuous Galerkin formulation will be presented to address this issue.

3 Discontinuous Galerkin formulation based on a lifting operator

Consider a partition $\mathcal{P}^h$ of the domain Ω containing n elements E_i, $i=1\rightarrow n$, such that $\bigcup_{i=1}^{n}\bar{E}_i=\bar{\Omega}$ and $\bigcup_{i=1}^{n}E_i=\tilde{\Omega}$. The union of all element edges is denoted by $\Gamma=\bigcup_{i=1}^{n}\partial E_i$, and the union of all internal element edges is denoted by $\tilde{\Gamma}=\Gamma\setminus\partial\Omega$. The trial and test function spaces on the mid-surface are defined as follows

$$U^h=\left\{\boldsymbol{u}^h\in[H^1(\Omega)]^3:u_j^h\in P^k(E_i),\;j=1\rightarrow 3,\;\forall\,E_i\in\mathcal{P}^h;\;\boldsymbol{u}^h|_{\Gamma^u}=\boldsymbol{g}^u\right\}, \quad (21)$$

$$W^h=\left\{\boldsymbol{w}^h\in[H^1(\Omega)]^3:w_j^h\in P^k(E_i),\;j=1\rightarrow 3,\;\forall\,E_i\in\mathcal{P}^h;\;\boldsymbol{w}^h|_{\Gamma^u}=\boldsymbol{0}\right\}, \quad (22)$$

where $P^k(E_i)$ are standard finite element shape functions of polynomial degree k. We adopt the jump and average definitions for a scalar function a on an edge e as follows: for an interior edge $e\in\tilde{\Gamma}$

$$[\![a_{,n}]\!]=a^{+}_{,\alpha}n^{+}_{\alpha}+a^{-}_{,\alpha}n^{-}_{\alpha},\qquad\qquad \langle a\rangle=\frac{1}{2}\left(a^{+}+a^{-}\right), \quad (23)$$

and for an exterior edge $e\in\partial\Omega$

$$[\![a_{,n}]\!]=a_{,\alpha}n_{\alpha},\qquad\qquad \langle a\rangle=a. \quad (24)$$

In the above equations, a denote values of the function on e of elements E and $E^{\pm}$, respectively, where $E^{\pm}\in\mathcal{P}^h$ denote two elements sharing the interior edge e; n_α and $n_\alpha^{\pm}$ denote the outward normal vector of elements E and $E^{\pm}$, respectively.

and $a^{\pm}$

Consider a lifting function space $\mathcal{R}^h$ as follows

$$\mathcal{R}^h=\left\{r_{\alpha\beta}\in L^2(\Omega):r_{\alpha\beta}(E_i)\in P^l(E_i)\;\forall\,E_i\in\;\mathcal{P}^h,\;r_{\alpha\beta}(E_i)=r_{\beta\alpha}(E_i)\right\}. \quad (25)$$

In addition, it is required that the space $\mathcal{R}^h$ must contain at least all the second derivatives of the function u_3^h on element interiors. For each element edge $e\in\tilde{\Gamma}\cup\Gamma^{\Theta}$, lifting operations are defined by: given $a\in H^1(\Omega)$, find $r^e_{\alpha\beta}\left(a\right),\,r^{e,g}_{\alpha\beta}\left(a\right)\in\mathcal{R}^h$ such that

$$\int_{\Omega}v^h_{\alpha\beta}\,r^e_{\alpha\beta}\left(a\right)\,d\Omega=-\int_{e}\left\langle v^h_{nn}\right\rangle[\![a_{,n}]\!]\;d\Gamma\qquad e\in\tilde{\Gamma}\cup\Gamma^{\theta},\;\forall\,v^h_{\alpha\beta}\in\mathcal{R}^h, \quad (26)$$

and

$$\int_{\Omega} v^h_{\alpha\beta}\, r^{e,g}_{\alpha\beta}\left(a\right)\, d\Omega = -\int_e \left\langle v^h_{nn}\right\rangle \left[\!\left[a_{,n}\right]\!\right]\, d\Gamma \qquad e \in \tilde{\Gamma},\ \forall\, v^h_{\alpha\beta} \in \mathcal{R}^h, \tag{27}$$

$$\int_{\Omega} v^h_{\alpha\beta}\, r^{e,g}_{\alpha\beta}\left(a\right)\, d\Omega = -\int_e v^h_{nn}\left(a_{,n} - g^{\theta}\right)\, d\Gamma \qquad e \in \Gamma^{\theta},\ \forall\, v^h_{\alpha\beta} \in \mathcal{R}^h, \tag{28}$$

where $v^h_{nn} = v^h_{\alpha\beta} n_\alpha n_\beta$. The integrals on the left-hand side of the above equations are performed over the elements sharing edge e. The lifting functions $r^e_{\alpha\beta}$ and $r^{e,g}_{\alpha\beta}$ are equal to zero for $e \in \Gamma^M$. Now, two functions $R_{\alpha\beta}\left(a\right)$ and $R^g_{\alpha\beta}\left(a\right)$ are defined as follows:

$$R_{\alpha\beta}\left(a\right) = \sum_{e\in\tilde{\Gamma}\cup\Gamma^{\theta}} r^e_{\alpha\beta}\left(a\right), \tag{29}$$

$$R^g_{\alpha\beta}\left(a\right) = \sum_{e\in\tilde{\Gamma}\cup\Gamma^{\theta}} r^{e,g}_{\alpha\beta}\left(a\right). \tag{30}$$

The proposed variational form for the thin shell problem involves: find $w^h \in W^h$ such that

$$B\left(\boldsymbol{w}^h, \boldsymbol{u}^h\right) = L\left(\boldsymbol{w}^h\right) \quad \forall \boldsymbol{w}^h \in \mathcal{W}^h, \tag{31}$$

where

$$\begin{aligned} B\left(\boldsymbol{w}^h, \boldsymbol{u}^h\right) = &\int_{\Omega} \gamma_{\alpha\beta}\left(\boldsymbol{w}^h\right) \mathcal{N}^{\alpha\beta}\left(\boldsymbol{u}^h\right) \sqrt{a}\, d\Omega \\ &+ \int_{\tilde{\Omega}} \left\{\kappa_{\alpha\beta}\left(\boldsymbol{w}^h\right) + R_{\alpha\beta}\left(w^h_3\right)\right\} \mathcal{M}^{\alpha\beta}_{\star}\left(\boldsymbol{u}^h\right) \sqrt{a}\, d\Omega \\ &+ \sum_{e\in\tilde{\Gamma}\cup\Gamma^{\theta}} \int_{\Omega} \frac{\eta t^3}{12}\, r^e_{\alpha\beta}\left(w^h_3\right)\, \mathcal{C}^{\alpha\beta\gamma\delta}\, r^{e,g}_{\gamma\delta}\left(u^h_3\right) \sqrt{a}\, d\Omega, \end{aligned} \tag{32}$$

and

$$L\left(\boldsymbol{w}^h\right) = \int_{\Omega} \boldsymbol{w}^h \cdot \boldsymbol{F} d\Omega + \int_{\Gamma^H} \boldsymbol{w}^h \cdot \boldsymbol{H}\, d\Gamma + \int_{\Gamma^M} \boldsymbol{\theta}\left(\boldsymbol{w}^h\right) \cdot \boldsymbol{M}\, d\Gamma. \tag{33}$$

In the above equations, $\mathcal{N}^{\alpha\beta}$ and $\mathcal{M}^{\alpha\beta}_{\star}$ denote the membrane stress and moment tensors on the mid-surface, which are written as

$$\mathcal{N}^{\alpha\beta}\left(\boldsymbol{u}^h\right) = t\mathcal{C}^{\alpha\beta\gamma\delta}\gamma_{\gamma\delta}\left(\boldsymbol{u}^h\right), \tag{34}$$

$$\mathcal{M}^{\alpha\beta}_{\star}\left(\boldsymbol{u}^h\right) = \frac{t^3}{12}\mathcal{C}^{\alpha\beta\gamma\delta}\left(\kappa_{\gamma\delta}\left(\boldsymbol{u}^h\right) + R^g_{\gamma\delta}\left(\boldsymbol{u}^h\right)\right), \tag{35}$$

and η is a positive number to provide stability of the formulation. The method allows to use standard C^0 Lagrange basis functions in terms of the displacement only. A weak continuity of normal derivative across element boundaries has been enforced by using the lifting operation to transforms jumps in the normal rotation across element boundaries into a field defined on element interiors. This enables the finite element solutions to be obtained in a straightforward implementation.

4 Numerical examples

The proposed formulation is subjected to some benchmark tests in this section, consisting of Scordelis-Lo roof, Pinched cylinder, and Hemisphere, which are popular in shell literatures. Shell elements with various orders of basis functions are used. Notably, the condition $l \geq k-2$, where l and k respectively are the order of the lifting function $P^l(E_i)$ and of the element shape function $P^k(E_i)$, is required. Here, the order $l = k-2$ will be adopted in all benchmark tests. Two types of triangle elements will be touched upon that are flat shell elements and curved shell elements.

Flat shell elements are constructed by combining membrane elements and plate bending elements together. Curved surfaces are now represented approximately by a surface of flat elements. Within an element, there exists no geometric curvature and no membrane-bending coupling effects. When curved elements are used, geometries of the considered shell problems are represented exactly by using proper mappings from two dimensional reference domains to the shell mid-surfaces and membrane-bending coupling effects are taken into account.

4.1 Scordelis-Lo roof

This model is very useful to check the correctly representing ability of elements in a complex states when both the membrane and bending strain energy contributions to the total energy are considerable. Geometry parameters of the roof is shown in Figure 2a with a rigid-support on two curved boundaries, free on two other straight boundaries, side length $L = 50\,m$, radius $r = 25\,m$, thickness $t = 0.25\,m$, open angle $\phi = 40^o$, Young's modulus $E = 4.32 \times 10^8 N/m^2$, and Poisson's ratio $\nu = 0$. A uniform gravity load $F = 90N/m^2$ is applied.

For this problem, a single chart is used to map a flat rectangular domain to the curve shell domain, see Figure 2b. The vertical displacement computed at the mid-point of the free edges is normalized using the reference solution $0.3024\,m$ given in [9]. As shown in Figure 3 are the results using quadratic flat-shell and curve-shell elements ($k = 2$) with different values of the penalty parameter η. As observed results, they all convert very well to exact solution. It is clear that flat-shell elements are 'softer'. The reason for this may be the lack of membrane-bending coupling effects in the flat-shell model. The convergence behaviour for cubic triangle elements ($k = 3$) is presented in Figure 4. Compared to the previous case, a faster convergence and a less sensitivity to the penalty parameter η are obtained. Observed results shown that presented elements are able to represent correctly the membrane and bending strains in a complex states.

4.2 Pinched cylinder

This problem tests the ability of the formulation to deal with inextentional bending states. The free-boundary cylinder shown in Figure 5a has the parameters: circumference length $L = 600\,mm$, radius $R = 300\,mm$, thickness $t = 3\,mm$, Young's modulus $E = 3 \times 10^6 N/mm^2$, and Poisson's ratio $\nu = 0.3$. Two opposing forces of $P = 1\,N$ are applied at the midway of the cylinder circumference.

A multi-mapping is used to generate the mid-surface of the cylinder, see Figure 5b. The reference solution $4.520 \times 10^{-4}\,mm$ given by Cirak et al. [10] has been used to

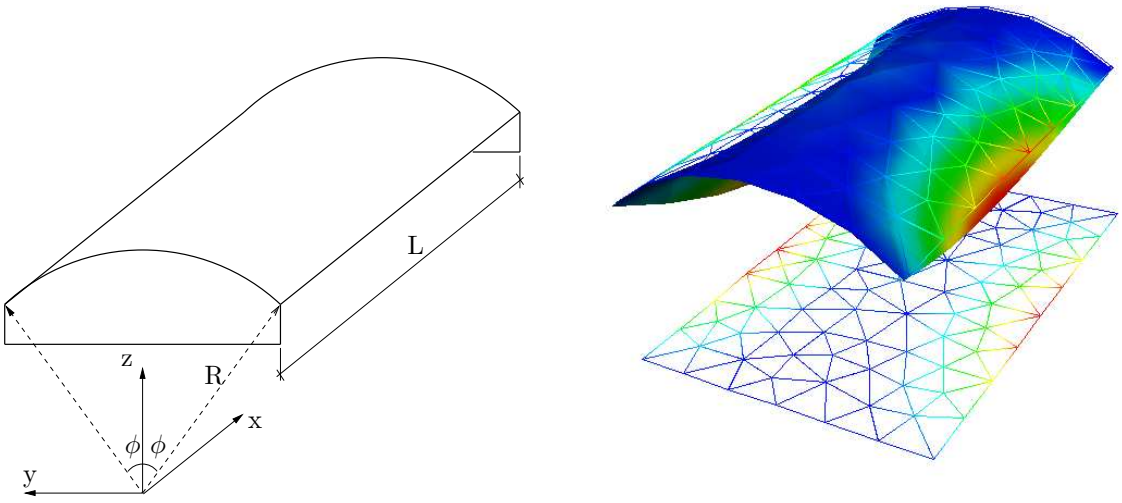

(a) (b)

Figure 2: Scordelis-Lo roof: (a) geometry; (b) reference domain (the flat grids), undeformed mid-surface (the curved grid), and deformed mid-surface.

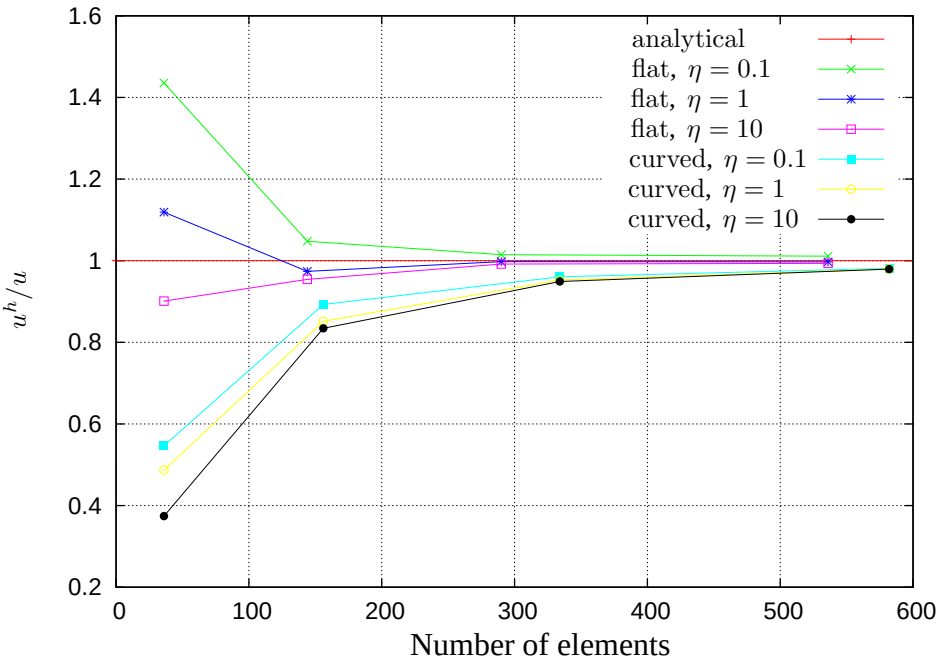

Figure 3: Scordelis-Lo roof: normalized displacement for the case $k = 2$ and $l = 0$ with various penalty values.

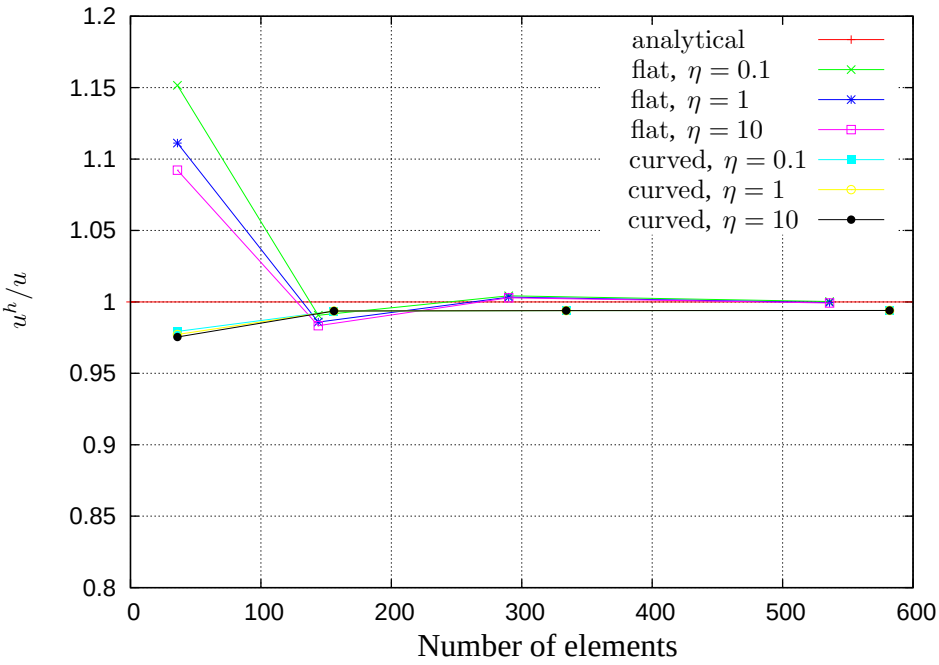

Figure 4: Scordelis-Lo roof: normalized displacement for the case $k = 3$ and $l = 1$ with various penalty values.

normalize the displacement at the loading points. Note that the reference solution is derived for an inextention cylinder with an assumption stating that all strain components in the mid-surface vanish. Again, flat shell and curved shell elements are used. Here we do not employ simmetric property and discretize the entire cylinder. Obtained results using quadratic shape functions are performed in Figure 6. As shown, implementation of quadratic flat elements reproduces a softer behaviour and a better convergence. In Figure 7 are the results for the case of cubic elements. Because obtained results are compared to an inextention reference solution, they are all showing a "softer" performance.

4.3 Hemisphere

Together the pinched cylinder, the hemisphere test is an obstact benchmark problem that is used to test inextentional bending in complex strain states. Parameters of the Hemisphere are: radius $R = 10\,m$, thickness $t = 0.04\,m$, Young's modulus $E = 6.825 \times 10^7 N/m^2$, and Poisson's ratio $\nu = 0.3$. The applied forces have a magnitude $F = 2\,N$ (see Figure 8a).

The deformed mid-surface of the hemisphere is shown in Figure 8b. The displacement at the loading points is normalized using the reference solution $0.0924\,m$ given in [9] . The results are shown in Figure 9 for the case of quadratic elements and in Figure 10 for the case of cubic elements. It is very clear that for the case of $k = 3$, curved-shell elements reproduce a much faster convergence compared to that by flat-shell elements.

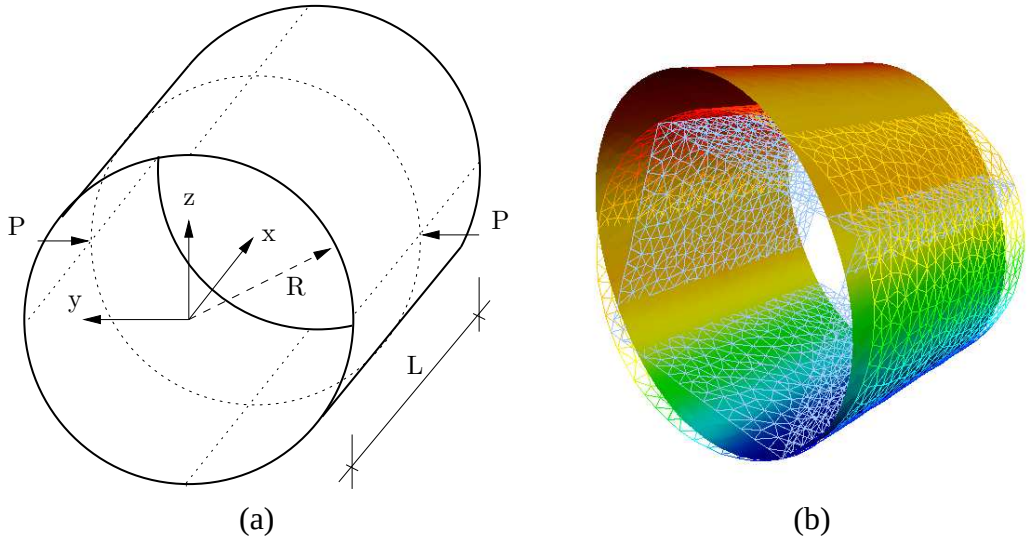

Figure 5: Pinched cylinder: (a) geometry; (b) reference domain (the flat grid), undeformed mid-surface (the curved grid), and deformed mid-surface.

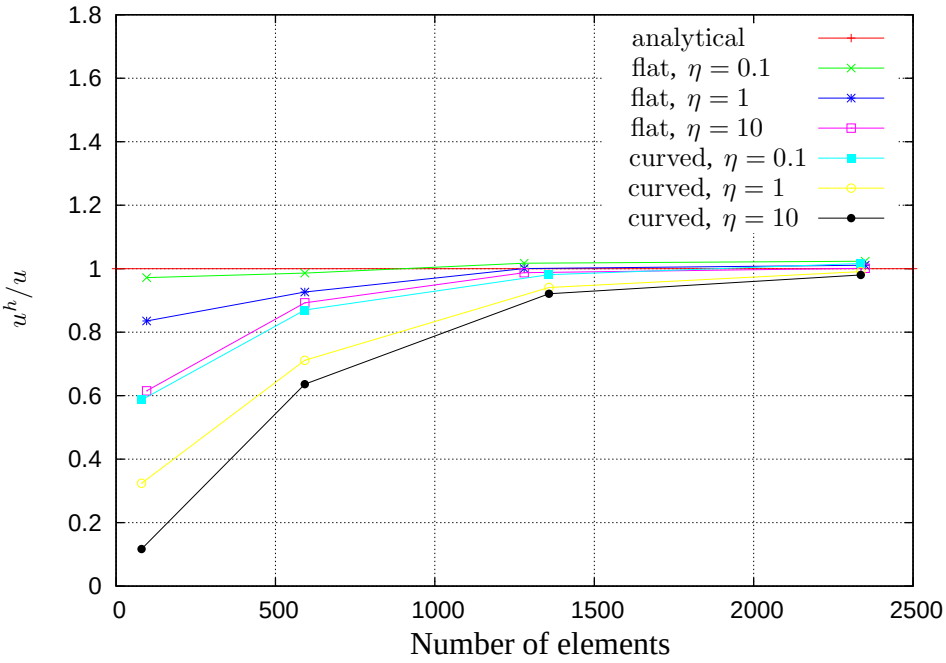

Figure 6: Pinched cylinder: normalized displacement for the case $k = 2$ and $l = 0$ with various penalty values.

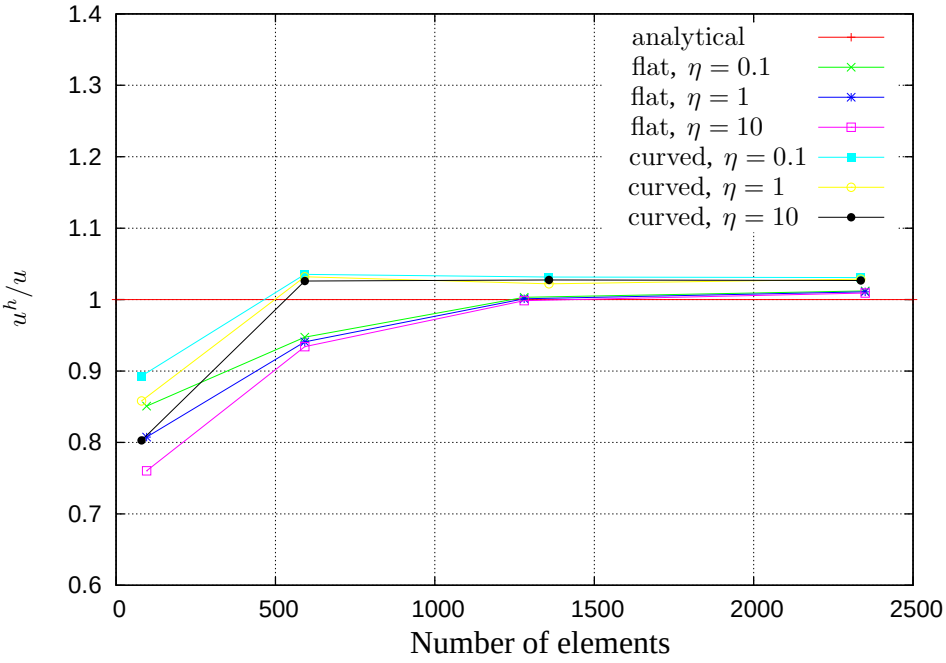

Figure 7: Pinched cylinder: normalized displacement for the case $k = 3$ and $l = 1$ with various penalty values.

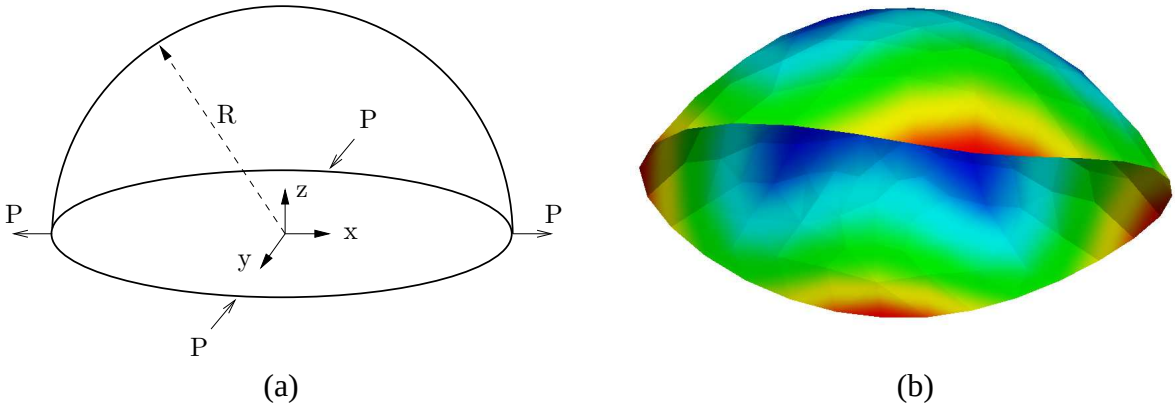

Figure 8: Hemisphere: (a) geometry; (b) deformed mid-surface.

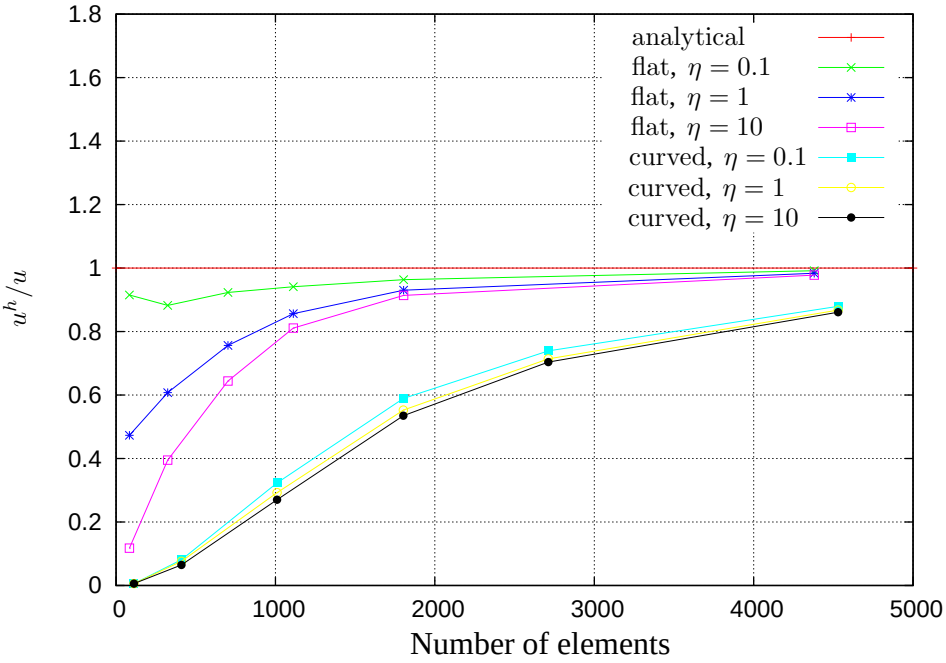

Figure 9: Hemisphere: normalized displacement for the case $k = 2$ and $l = 0$ with various penalty values.

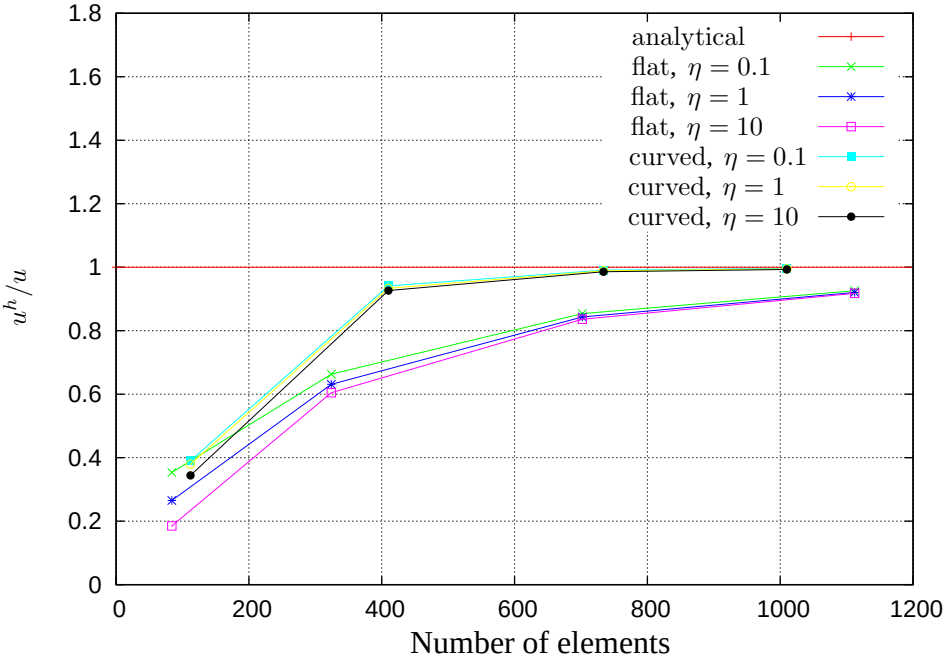

Figure 10: Hemisphere: normalized displacement for the case $k = 3$ and $l = 1$ with various penalty values.

5 Conclusion

The discontinuous Galerkin formulation presented here allows to simulate Koiter's thin shell models by using standard C^0 Lagrange basis functions with displacement degrees of freedom only. To weakly enforce a C^1 continuity, jumps in the normal rotation across element boundaries have been lifted to a defined interior field. Together with the unconditionally stability condition, the absence of rotation degrees of freedom make the approach particularly attractive for simulating of thin shells.

Flat shells: there exists no geometric curvature and no membrane-bending coupling effects. This this a major disadvantage of the model. However, the finite element implementation using this approach is simple because difficulties relating to the curved shell geometry are delivered. Curved shells: exact geometric representation, membrane-bending coupling effects.

Acknowledgments

NTD gratefully acknowledges the support of the Vietnamese Ministry of Education and Training (VMOET) and the TUD Management Centre for International Cooperation (CICAT) and GNW acknowledges the support of the Netherlands Technology Foundation STW, applied science division of NWO and the technology programme of the Ministry of Economic Affairs.

References

[1] M. Bernadou. *Finite Element Methods for Thin Shell Problems*. John Wiley & Sons, New York, 1996.

[2] D. Chapelle and K. J. Bathe. *The Finite Element Analysis of Shells - Fundamentals*. Springer, 2003.

[3] G. Engel, K. Garikipati, T. J. R. Hughes, M. G. Larson, and R. L. Taylor. Continuous/discontinuous finite element approximations of fourth-order elliptic problems in structural and continuum mechanics with applications to thin beams and plates, and strain gradient elasticity. *Computer Methods in Applied Mechanics and Engineering*, 191(34):3669–3750, 2002.

[4] T. J. R. Hughes and K. Garikipati. On the continuous/discontinuous Galerkin (CDG) formulation of Poisson-Kirchhoff plate theory. In K. M. Mathisen, T. Kvamsdal, and K. M. Okstad, editors, *Computational Mechanics - Theory and Practice*. CIMNE, Barcelona, 2004.

[5] G. N. Wells and N. T. Dung. A C^0 discontinuous Galerkin formulation for Kirchhoff plates. *Computer Methods in Applied Mechanics and Engineering*, accepted.

[6] F. Bassi and S. Rebay. A high-order accurate discontinuous finite element method for the numerical solution of the compressible navier–stokes equations. *Journal of Computational Physics*, 131(2):267–279, 1997.

[7] F. Brezzi, G. Manzini, D. Marini, and A. Russo. Discontinuous Galerkin approximations for elliptic problems. *Numerical Methods for Partial Differential Equations*, 16(4):365–378, 2000.

[8] W. T. Koiter and J. G. Simmonds. *Foundations of shell theory*. Delft University of Technology, the Netherlands, 1972.

[9] T. Belystchko, H. Stolarski, and W. K. Liu. Stress projection for membrane and shear locking in shell finite elements. *Computer Methods in Applied Mechanics and Engineering*, 51:221–258, 1985.

[10] F. Cirak, M. Ortiz, and P. Schroder. Subdivision surfaces: a new paradigm for thin-shell finite-element analysis. *International Journal for Numerical Methods in Engineering*, 47(12):2039–2072, 2000.